Interchangeable Stage and Probe Mechanisms for Microscale Universal Mechanical Tester

Joseph J. Brown, *Member, IEEE*, Dmitriy A. Dikin, Rodney S. Ruoff, and Victor M. Bright, *Senior Member, IEEE*, *Fellow, ASME*

***Abstract*—A microfabricated mechanical test platform has been designed, fabricated, and operated. This system consists of a reusable chip capable of large-displacement actuation, which interfaces to a test coupon chip compatible with synthesis conditions for many nanomaterials. Because only normal forces are used for mechanical interfacing, the two chips are not permanently connected, allowing exchange of the test coupon chips. The actuated test platform chip contains a thermal actuator driving a compliant displacement amplification transmission, and a bulk-micromachined well in which the test coupon chips may be placed and removed. The displacement amplification structure provides 40 μm of output displacement, extending a probe over the well and into contact with the test coupon. The test coupon contains compliant structures that are actuated by the probe from the test platform. [2011-0279]**

***Index Terms*—Assembly, compliant structure, interchangeable, microactuator, micromanipulator, universal mechanical tester.**

I. Introduction

THIS PAPER reports the development and operation of a new micromechanical probe and stage system consisting of a reusable actuated test platform chip in combination with interchangeable test coupon chips capable of withstanding high-temperature nanomaterial synthesis conditions (Fig. 1). This design is intended as the basis for a microfabricated universal mechanical tester compatible with electron microscopes and other analytical tools for mechanical property cross-correlation experiments. Universal mechanical testers, also known as universal testing machines, are commonly used for mechanical characterization of material specimens. These machines perform tensile, compressive, and bending tests, depending on the setup of test specimens. Such test machines generally consist of mechanisms for supporting and applying load to material specimens, and means of detecting the force and strain experienced by the specimen. In order to serve as a component of a microscale universal mechanical tester, a micromechanical test stage, suspended from compliant flexures, was defined on a "test coupon" microchip. Actuation was achieved with a surface-micromachined probe on an additional chip that contacted the removable test coupon.

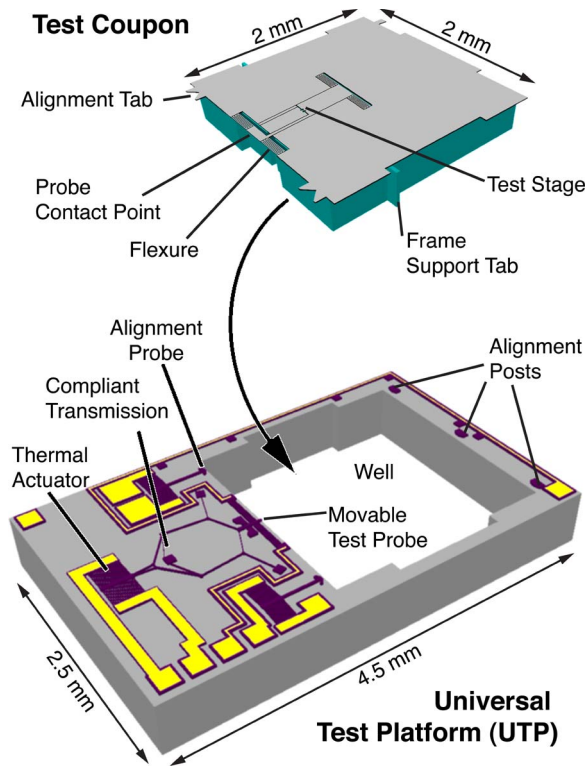

Fig. 1. UTP and test coupon dual-chip system. Interfacing between coupon and UTP was designed as a loose fit with 10 μm in-plane fit allowance.

The central motivation of this work was the development of microdevices for tensile testing, but this derived from a broader goal to demonstrate a flexible adaptable platform for miniaturization of laboratory instrumentation for experimentation with solid structures. The systems presented here were designed to be adapted and repurposed to additional applications. Microsystems and nanosystems for analysis and manipulation of solid materials have produced many scientific and engineering advances [1]–[3], but more work is needed for these systems to develop impacts and uses comparable to those achieved by the

Manuscript received September 19, 2011; revised October 20, 2011; accepted November 8, 2011. Date of publication December 27, 2011; date of current version April 4, 2012. This work was supported by the DARPA Center on Nanoscale Science and Technology for Integrated Micro/Nano-Electromechanical Transducers (iMINT) through the DARPA N/MEMS S&T Fundamentals Program (Award #HR0011-06-1-0048). The work of J. J. Brown was supported by a National Science Foundation Graduate Research Fellowship. Subject Editor R. T. Howe.

J. J. Brown and V. M. Bright are with the Department of Mechanical Engineering and the DARPA Center on Nanoscale Science and Technology for Integrated Micro/Nano-Electromechanical Transducers (iMINT), University of Colorado, Boulder, CO 80309-0427 USA (e-mail: joseph.j.brown@colorado.edu; victor.bright@colorado.edu).

D. A. Dikin is with the Department of Mechanical Engineering, Northwestern University, Evanston, IL 60208 USA (e-mail: d-dikin@northwestern.edu).

R. S. Ruoff is with the Department of Mechanical Engineering, University of Texas at Austin, Austin, TX 78712-0292 USA (e-mail: r.ruoff@mail.utexas.edu).

Color versions of one or more of the figures in this paper are available online at http://ieeexplore.ieee.org.

Digital Object Identifier 10.1109/JMEMS.2011.2177071

field of microfluidics, which has become key to accelerating progress in biology and microscale chemistry [4]–[6].

Nanomechanical experiments face spatial constraints that require simplification of experiments or greater intricacy of the experimental apparatus in the volume available. For example, specimen holders for transmission electron microscopes (TEMs) typically impose design constraints of a few millimeters in the directions perpendicular to the holder axis, severely restricting the range of motion available to manipulator structures. One-dimensional straining stages for TEMs are well established, and a number of these are commercially available and used experimentally [7], [8]. Some interchangeable test coupons have been developed for direct interfacing from TEM straining stages, for instance, by means of two pins passing through holes at each end of a chip [9]–[11]. Several other examples of modified TEM stages have been created, most notably for applications such as electrical conductivity measurements [12]–[14], scanning probe microscopy [15], and nanoindentation probing within a TEM [16], [17]. With additional design complexity, manipulators with multiple degrees of freedom have been demonstrated for operation within TEM and scanning electron microscope environments [18]. An alternative approach to increase the sophistication of nanomechanical experiments is to perform straining with microsystems [19], [20].

Because MEMS allow operation in physically constrained spaces and can operate with multiple electrical signals connected to MEMS components, many opportunities exist for their use in investigations of mechanical properties of materials [1]–[3]. Mechanical characterization of structures with nanoscale dimensions has been achieved with integrated microfabricated systems [19], [21]–[26]. In these designs, comb drives and thermal actuators were used to drive motion in MEMS mechanical testers, and displacement and force measurements were achieved by image analysis, correlation of motion with input electrical power, or capacitive sensing [19], [21], [27], [28].

Even with use of microscale mechanical testing systems, placement of a nanomaterial specimen on a tensile stage remains a significant challenge. Simplifying manipulation of microscale and nanoscale specimens may increase the rate of experimentation. Techniques for manipulation of individual nanotubes and nanowires (NWs) include deposition from liquid dispersions [29]–[31] and dielectrophoretic assembly from suspension to bridge a specified gap [32], [33], and placement using micromanipulator probes [34], [35]. Micromanipulators present the significant risk of damaging test systems, as do the menisci from liquid suspensions [31]. Flip chip transfer of carbon nanotubes (CNTs) to test structures allows integration of individual CNTs into larger microsystems, but this technique risks microsystem damage and difficulty in specimen alignment [36]. Specified CNT growth has been achieved by depositing catalyst at one anchoring location and applying environmental conditions that promote the growth of nanotubes at the catalyst particles [37]–[39]. The major disadvantage of this is that not all microsystems will tolerate the typically > 800 °C temperatures required for CNT growth [32], [37], [38].

Some opportunities for speeding specimen preparation derive from separation of tester actuation from specimen mounting. This enables processes such as dielectrophoretic NW placement or CNT chemical vapor deposition, eliminating the need for micromanipulation of individual nanoscale fibers. Within a tester device, physical separation of test specimens from actuation and sensing components may reduce the potential for damage during specimen placement operations. In addition, supporting microscale and nanoscale specimens on microfabricated test coupons enables laboratory macroscale manipulation of the specimens, substituting handling of specimens with handling of a test coupon. Finally, devices that allow probing from a direction normal to a specimen may be useful for property cross-correlation measurements such as piezoresistive, optomechanical, or radio frequency electromechanical tests. The devices presented in this paper were developed in pursuit of these opportunities for MEMS-based material testers: faster specimen preparation, lab-scale nanospecimen handling, and new investigations of associated physical properties in nanomaterial specimens.

II. System Designs

Systems of "universal test platform" (UTP) and "test coupon" microchips (Fig. 1) were designed to generate forces at a microfabricated tensile test stage within one or two orders of magnitude of the force estimated for nanofiber fracture ($\sim$400 μN for GaN NWs with $\sim$300 nm diameter [21] and $\sim$10 μN for CNTs with $\sim$100 nm diameter or for a bundle of CNTs with smaller diameters [35]). The designs used uniaxial motion in order to minimize potential sources of error due to misalignment, such as bending moments and specimen clamp failure. The interface was designed as a temporary mechanical connection in order to allow exchange of test coupons. Constraining actuation to in-plane motion allowed out-of-plane access to the test stage by optical and electron microscopy and may enable further characterization methods, such as electrical measurements, or optical fluorescence tests. Voids in the specimen-supporting area of the coupons, in combination with the wells in the test platform chips, enabled optical transmission and transmission electron microscopy.

A. Interfacing and Assembly

The mechanical interface between the coupon and the UTP was designed to allow for reuse of the UTP and variation of the test coupon designs. All mechanical interfacing was performed with normal forces in order to minimize stiction, wear, and distortion of measurements due to mechanical slipping. In-plane motion was achieved by confining actuated motion to the plane of a device layer anchored to a fabrication substrate. Reliable interfacing between the UTP probe and the suspended stage required that the coupon and UTP test system accommodate vertical misalignment. The contacting microprobe must contact the edge of the coupon device layer. The coupon aligned vertically to the test platform probe simply by resting on the test platform. The bulk part of the test coupon was inserted into a well formed within the UTP chip. Protruding tabs formed in the test coupon device layer rested on the surface of the test

platform, and the coupon was held in place by gravity. This approach to vertical self-alignment was designed to function on the condition that the thickness of the coupon device layer (about 10–30 μm) is thicker than that of the sacrificial layer removed from the test platform (1 μm). Because test coupons were placed face up, the coupon front side remained available for optical and electrical access.

Several passive in-plane alignment mechanisms were designed. These were posts and springs that abutted tabs on the coupon. In addition, an active alignment mechanism was designed, wherein actuators would push circular probes into V-shaped tabs, pushing the coupon against posts at the back of the well and laterally aligning the coupon so that both edges of the V would contact the circular tab.

The two-chip system, UTP and coupon (Fig. 1), was designed to have a loose fit with sufficient clearance to accommodate dimensional variations resulting during fabrication and placement. Contact between the chips occurred between the device layers of each chip. Design of the UTP deep well allowed the bulk portion of the test coupons to fit with an allowance of 50 μm in the X- and Y-directions. In the device layers, the designed fit allowance was 10 μm in X and Y, allowing 0.5% of the overall dimension of the 2 mm coupon for manufacture imprecision and placement misalignment. In practice, the fit allowances were somewhat larger because the deep etch processes used in coupon and UTP chip fabrication overetched the vertical walls in the coupon and test platform devices.

In order to create a test probe capable of providing sufficient force (> 400 μN) for nanomaterial fracture and sufficient displacement (> 10 μm) to accommodate the fit allowance, displacement amplification transmission systems were designed, and thermal actuators were chosen to drive these amplification systems. The displacement amplification systems were designed by considering arrangements of bending beams and simulating their maximum displacement and maximum force outputs using Coventorware software [40]. In order to prevent frictional wear and unpredictable stiction behavior, the displacement amplification systems were not based on pinned joints, and all anchor points were clamped. By constraining the internal stresses to less than the tensile strength of Si and seeking maximum force and displacement outputs, the optimized beam mechanisms shown in Fig. 2 were found through design and simulation. Extra springs were included as a design variation at the end of probe designs as potential piezoresistive displacement sensors.

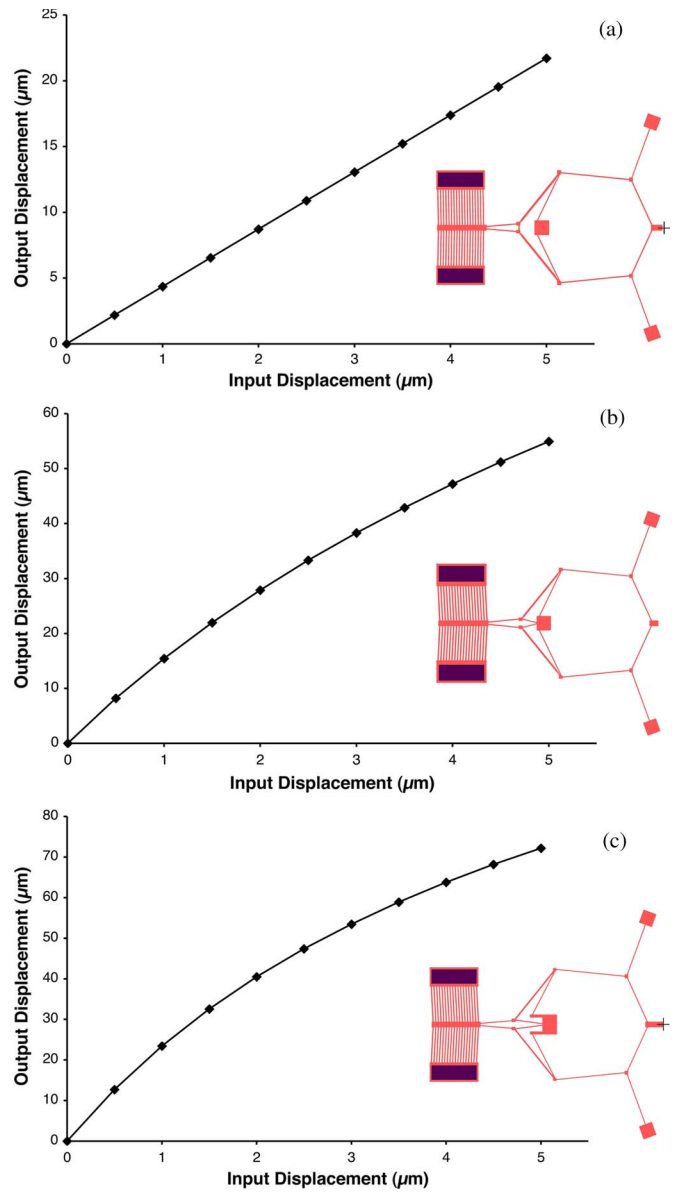

Fig. 2. Three displacement amplification transmission designs that were implemented in the UTP, showing simulation results and insets of the transmission structures attached to thermal actuator drives. Designs were created in L-edit software [41] and simulated using Coventorware software [40]. (a) Transmission Design 1, with amplification ratio of 4.34 : 1 at 5 μm input. (b) Transmission Design 2, with amplification ratio of 11.0 : 1 at 5 μm input. (c) Transmission Design 3, with amplification ratio of 14.4 : 1 at 5 μm input.

B. Universal Test Platform (UTP)

The Universal Test Platform (UTP) was designed as an actuated microfabricated device for driving mechanical components on the test coupon chips. The test platform design was based on the use of a microfabricated probe for actuation of the test coupon and structures for the mechanical alignment and interfacing between the two chips (Fig. 1). The microprobe was designed as a bending beam thermal actuator coupled to a compliant transmission structure for displacement amplification (Fig. 2). Six UTP design variations were generated and fabricated, with dimensions of 4.5 mm × 4 mm, 3.5 mm × 4 mm, and 2.5 mm × 4 mm (Fig. 3). These layouts placed the tensile test stages exactly at the center of the UTP chip. The UTP thermal actuators were driven by a Darlington transistor pair acting as a current sink controlled by an op-amp current control loop, itself driven by a National Instruments NI-6009 data acquisition system controlled by a custom MATLAB graphical user interface [42].

C. Test Coupon

The test coupon chips (Fig. 4) were conceived as specimen holders on which nanowire or nanotube specimens could be

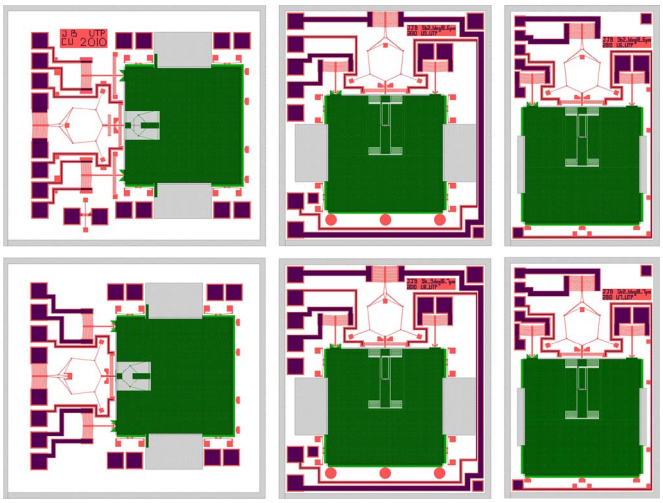

Fig. 3. Six different UTP chip designs. Dimensions of the different layouts were (left) 4.5 mm × 4 mm, (center) 3.5 mm × 4 mm, and (right) 2.5 mm × 4 mm. For all designs, passive alignment structures present general positioning of test coupons (large, square, shaded regions), and actuated mechanical probes extend from the test platform chips to contact the test coupons.

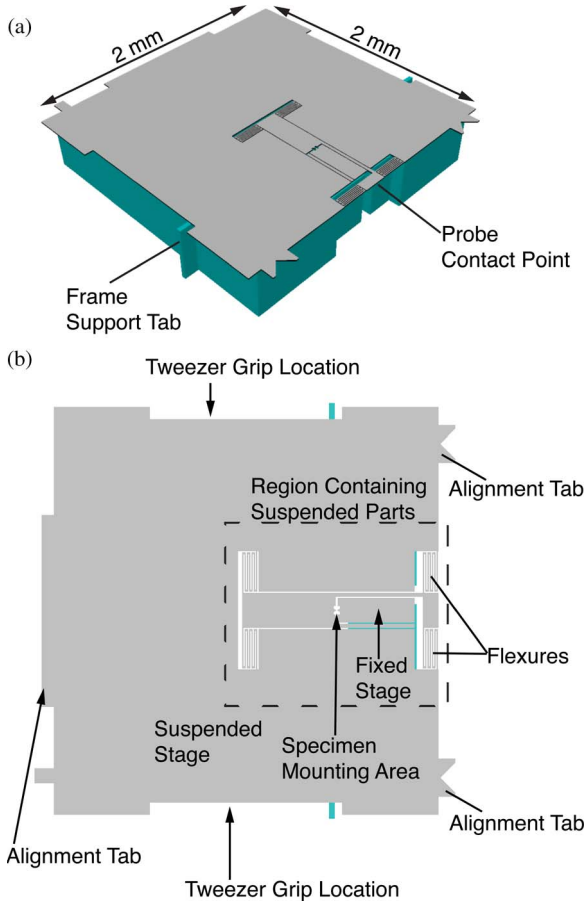

Fig. 4. Illustration of Test Coupon Design A. (a) Oblique view. (b) Top view.

placed or grown. Coupons consisted of a device layer that was a small region of a larger chip, 2 mm × 2 mm in size, used for handling in a laboratory. This was about the minimum size for coupon chips to be easily manipulated by hand with tweezers. The active test area on these chips was restricted to 500 μm × 500 μm due to the lithographic constraint of a beam

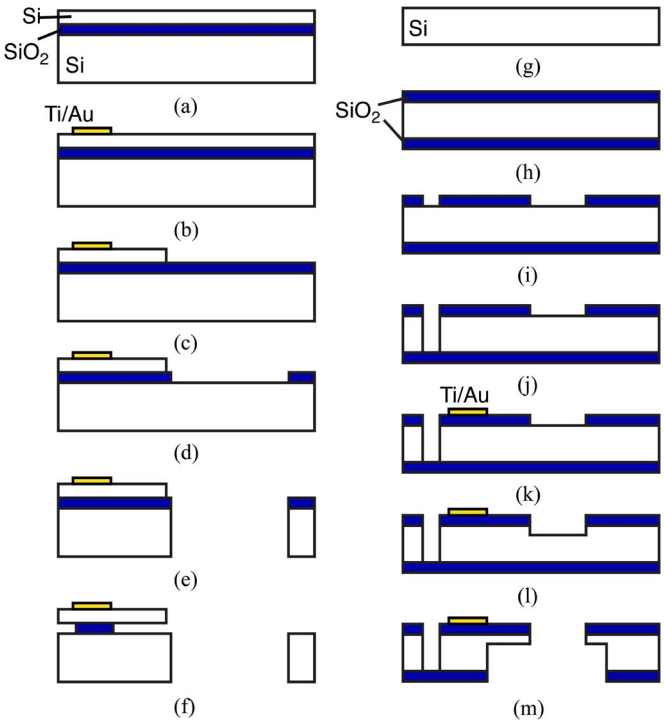

Fig. 5. Fabrication processes. (a)–(f) Process flow for UTP fabrication. (g)–(m) Process flow for test coupon fabrication.

length to width aspect ratio of less than 300:1 and due to the need for flexures that were thicker than they were wide in order to prevent out-of-plane vibrations and stabilize in-plane motion. Layouts were designed with symmetric flexure placement about the axis of motion in order to provide more robust stabilization of uniaxial motion than could be achieved with asymmetric layouts. Test coupons were fabricated from silicon substrates and were designed to tolerate high-temperature (e.g., ~800 °C) environments to enable CNT growth. Although tensile motion was targeted for proof-of-concept demonstrations, the test coupon compliant mechanisms may be adapted to alternative mechanical test operations such as bending and compression tests.

In order to allow for several-micrometer deformation of a test specimen, test coupons were designed to include fixed and moving stages for supporting the specimen and a network of supporting flexures to connect the moving stages to the fixed portions of the chips. Attachment of a test specimen would modify the effective spring constant k_{eff} of these networks, essentially coupling the stiffness k_0 of the specimen in parallel to the stiffness k_s of the coupon suspension (1). In coupons designed for tensile testing, measurement of force F and displacement d at the UTP allows observation of k_{eff} and extraction of the tensile load F_0 (2).

$$k_{\text{eff}} = k_s + k_0 \tag{1}$$

$$F_0 = F - k_s d = (k_{\text{eff}} - k_s)d. \tag{2}$$

III. Fabrication

The UTP chips were fabricated according to the process shown in Fig. 5(a)–(f). Fabrication began with a

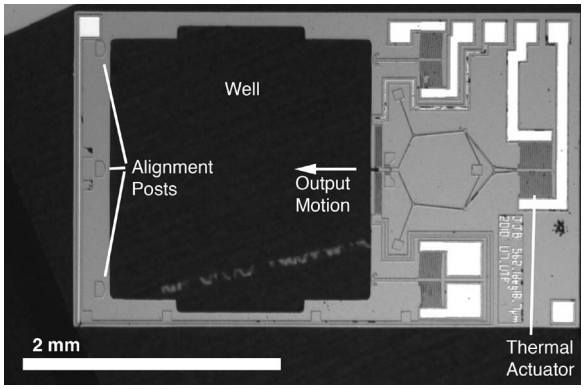

Fig. 6. Example of fabricated 2.5 mm × 4 mm UTP chip with Transmission Design 1 [Fig. 2(a)]. Chip thickness: 500–530 μm. The arrow indicates the location and direction of the UTP probe output motion.

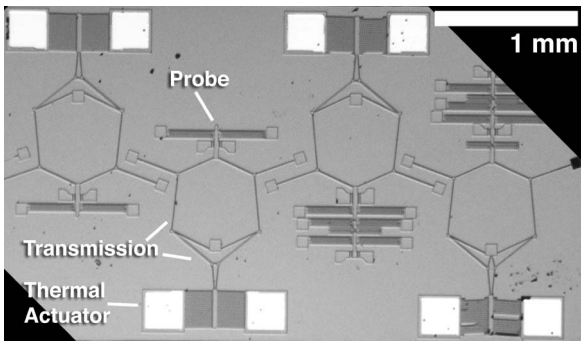

Fig. 7. Optical microscope image of a portion of a fabricated array of displacement amplification test structures. The compliant transmission designs visible in this image are Transmission Design 1 [Fig. 2(a)] and Transmission Design 2 [Fig. 2(b)].

system-on-insulator (SOI, $Si/SiO_2/Si$) wafer [Fig. 5(a)]. A metal layer (Au on Ti for adhesion) was evaporated onto the wafer and patterned with lift-off [Fig. 5(b)]. The Si device layer was patterned with deep reactive ion etching (DRIE) [Fig. 5(c)]. A deep well was patterned by using reactive ion etching (RIE) to clear the SiO_2 [Fig. 5(d)], followed by DRIE for removal of $\sim$500 μm of Si completely through the SOI handle wafer layer [Fig. 5(e)]. Wet etching with hydrofluoric acid, followed by supercritical CO_2 drying, was used to release moving parts [Fig. 5(f)]. UTP fabrication was performed on only the front side of wafers. Deep etching preempted the need for dicing. By designing deep wells surrounding the UTP chips, etching completely through the UTP wafer separated all the chips from each other. Fig. 6 shows an example of a fabricated UTP chip.

Test coupon fabrication proceeded according to the process shown in Fig. 5(g)–(m). This process began with a double-side polished Si wafer [Fig. 5(g)], onto which 1 μm thickness thermal oxide was grown [Fig. 5(h)]. The oxide layer was patterned and etched using RIE [Fig. 5(i)], and alignment holes were machined completely through the wafer using DRIE [Fig. 5(j)]. Metal (Ti/Au) was evaporated onto the wafer and patterned with lift-off [Fig. 5(k)], after which DRIE was used to pattern the silicon devices on the front side [Fig. 5(l)]. At this point, the wafer front side was mounted to a backing wafer using wax (Crystalbond 509), and deep wells were etched on

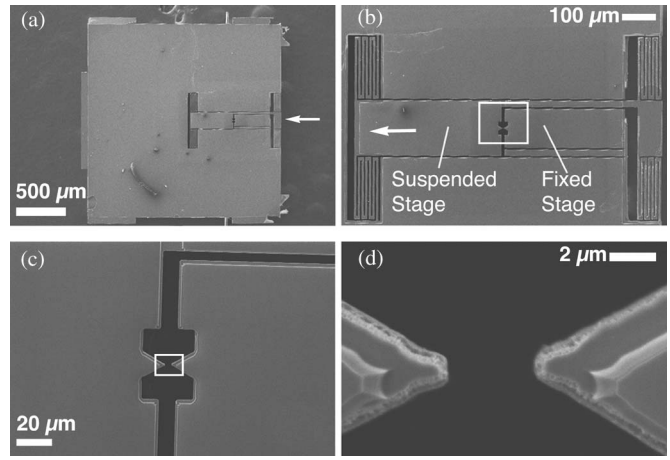

Fig. 8. Magnification series of Test Coupon Design A. (a) Entire 2 mm × 2 mm coupon. The arrow in (a) indicates the location of contact from the UTP probe. (b) View of the entire test stage mechanism, including the fixed and suspended mechanical stages, and the flexures used to hold the suspended stage. The rectangle in (b) indicates the region shown in image (c). The arrow in (b) indicates the direction of motion of the suspended test stage. (c) View of the test stage region defined for anchoring nanomaterial specimens, such as NWs or CNTs. The rectangle in (c) indicates the region shown in image (d), which is the optimal location for placement of tensile specimens. (d) View of smallest gap between the fixed and moving stages.

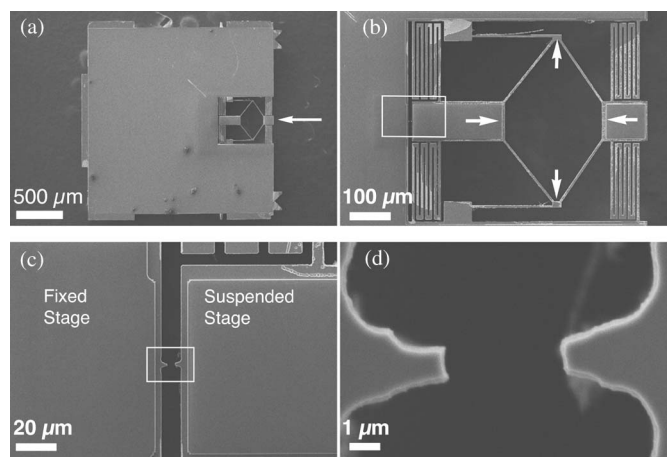

Fig. 9. Magnification series of Test Coupon Design B. (a) Entire 2 mm × 2 mm coupon. The arrow in (a) indicates the location of contact from the UTP probe. (b) View of the entire suspended test stage mechanism. The rectangle indicates the test stage region shown in (c). The arrows in (b) indicate the direction of motion of the suspended test stage and other parts of the compliant mechanism. (c) View of the test stage region defined for anchoring nanomaterial specimens, such as NWs or CNTs. The rectangle encloses the stage gap that is shown in (d). (d) View of smallest gap between the fixed and moving stages.

the back side to define coupon chips and their support frame [Fig. 5(m)]. The wafers were separated by soaking in acetone, and the coupon wafer was cleaned using an O_2 asher.

Back-side processing of the coupon wafer was required in order to create the suspended tabs that allowed alignment in the UTP. The deep etching steps necessitated supporting the coupon wafer on a backing wafer. Alignment to precision within ± 15 μm was achieved using holes micromachined completely through the wafer [Fig. 5(j)]. In order to support and separate the coupons during machining, each coupon was surrounded by a support frame machined from the coupon wafer. Tabs (Fig. 4) defined during the back-side processing step

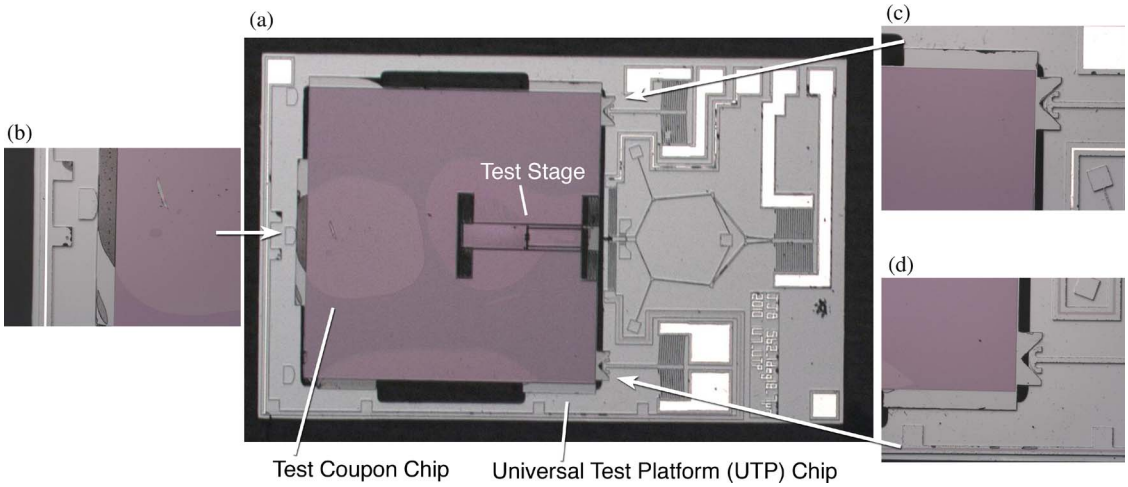

Fig. 10. Passive interfacing of a test coupon chip (Coupon Design A, Fig. 8) in a 2.5 mm × 4 mm UTP chip. (a) Optical image of a test coupon chip fitted into a UTP chip. (b)–(d) Magnified optical images of some of the points of XY passive alignment.

attached each coupon to the support frame. After processing, coupons were mechanically removed from the support frame by pressing on the coupons with tweezers.

IV. Characterization

A. Probe and Actuator Operation

In addition to the UTP designs (Fig. 6), arrays of actuator test designs were fabricated. Fig. 6 shows an example of a fabricated UTP chip, and Fig. 7 shows a portion of an array used for testing of actuators and transmissions. All three displacement amplification mechanisms (Fig. 2) capable of > 30 μm displacements succeeded in transferring motion to the probe ends. The thermal actuators operated at approximately 1 W of input power in air: ~5 V, 220 mA, DC.

B. Test Coupons

Two test coupon designs that were actuated using the UTP systems are shown in Figs. 8 and 9, and both were shown to be robust to liquid and high-temperature environments. As part of a handling test for potential nanomaterial sample mounting such as NW dielectrophoresis or CNT catalyst deposition, coupons were repeatedly immersed in isopropanol and dried in air without damage. Coupons were also demonstrated to survive heating to 800 °C in N_2 without damage.

The compliant mechanism in Coupon Design A (Fig. 8) was most effective for mechanical operation in the UTP. In this design, the suspended stage was connected by four flexures to the bulk of the test coupon. External actuation increased the size of the gap defined between the suspended stage and a nearby fixed stage. The compliant mechanism in Coupon Design B (Fig. 9) demonstrated reversing motion. The motion of the test stage was in the opposite direction of the motion applied with the UTP probe. External actuation moved a contact region toward the center of the test coupon, pushing two connecting regions away from each other. These connecting regions then pulled on a suspended test stage, separating it from the fixed region of the test coupon.

C. Three-Dimensional Interface Between Microfabricated UTP and Coupon Chips

Test coupon chips were assembled (Fig. 10) into the test platform well by hand using tweezers. They were easily removed either by tweezers or by gravity when the UTP was inverted. The tabs protruding from the coupon chips sometimes initially rested upon the device layer structures in the UTP. Light tapping on the surface supporting the UTP provided sufficient energy to allow the coupons to reposition themselves so that the tabs rested upon the UTP handle layer. Out-of-plane alignment (Z-direction) was achieved by contact between the coupon alignment tabs and the UTP handle layer. In-plane (X, Y, and θ) alignment was achieved by interaction of the coupon alignment tabs with structures patterned in the UTP device layer. In order to prevent damage to the UTP test probe and possible disturbance to the coupon test stage during placement of coupons in the UTP, the system was designed so that the UTP test probe would move 24 μm before contacting the test coupons. Operation on some fabricated devices required as much as 32 μm of probe motion before coupon contact (Fig. 11), indicating that the fabrication processes added 8 μm to the fit allowances, for some devices.

Over 40 μm of motion was obtained from the UTP probe (Fig. 11), and more than 5 μm of displacement was obtained for the test stage in Coupon Design A using actuation from a UTP probe (Figs. 11 and 12). Measurement and calibration of in-plane forces of MEMS mechanical testers can be performed using the characterization of springs within the testers [43], [44]. The test coupon suspension springs were used to indicate the real force output achievable with the UTP probe system. Fig. 13 shows that over 40 μm of output motion may be provided using an alternative transmission design (refer to Fig. 2 for transmission designs, Fig. 13 for Transmission Design 3, and Fig. 11 for Transmission Design 1). Furthermore, Fig. 13 verifies that the presence of a test coupon adds additional stiffness to the probe system output displacement, thereby reducing the displacement for a given current input. In Fig. 13, a UTP chip using Transmission Design 3 (Fig. 2) and the UTP design shown at the bottom left in Fig. 3 achieved 20 μm of

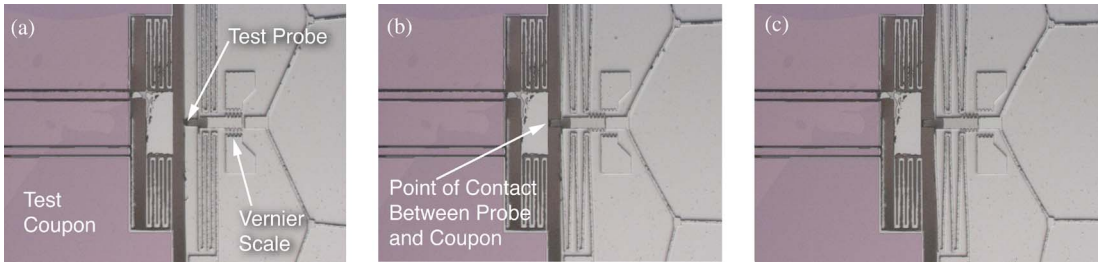

Fig. 11. Demonstration of UTP probe actuation of test coupon in magnification of the chips shown in Fig. 10. (a) Before actuation. (b) UTP probe in contact with coupon, after 32 μm of probe motion. (c) UTP probe has moved 40 μm, as indicated by the vernier scale, and has actuated the coupon.

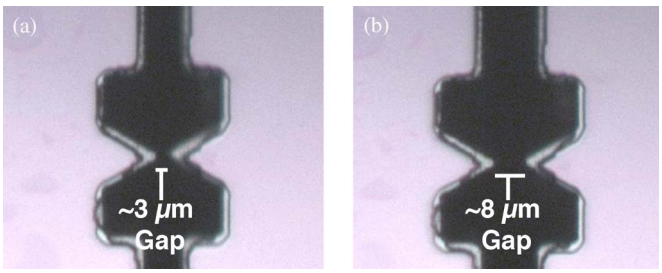

Fig. 12. Coupon Design A tensile stage. (a) Before operation, gap between sample mounting points ≈ 3 μm, as shown in Fig. 8(d). (b) After stage actuation, the gap was larger, with the gap between sample mounting points ≈ 8 μm.

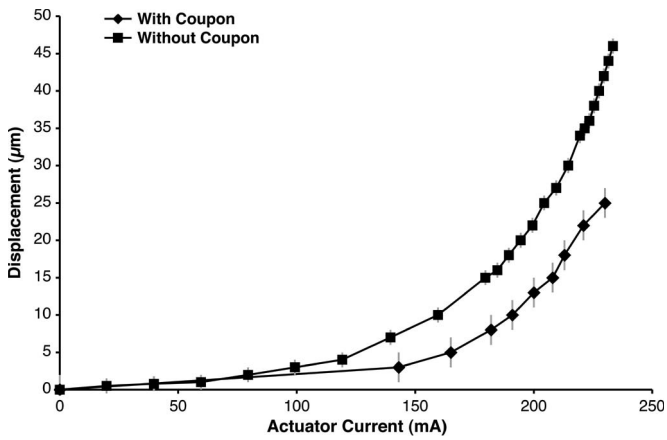

Fig. 13. Displacement versus actuator input current measured for a UTP chip with Transmission Design 3 (refer to Fig. 2), with and without a test coupon (Coupon Design A, Fig. 8) loaded. In order to obtain an estimate of the maximum force available experimentally from this actuator and transmission system, this test coupon was set up in contact with the UTP probe at the start of the test. Additional material was inserted between the coupon and the UTP alignment posts in order to backstop the coupon and push it in contact with the UTP probe.

displacement in actuation of the test coupon suspended stage with designed 55 N/m spring stiffness. Therefore, at least 1 mN of force $(20\ \mu\text{m} \times 55\ \text{N/m} = 1.1\ \text{mN})$ was applied by the probe to the suspended stage. Applying similar analysis to Fig. 11, Transmission Design 1 (Fig. 2) was capable of at least 440 μN of force output $(8\ \mu\text{m} \times 55\ \text{N/m} = 440\ \mu\text{N})$.

V. Conclusion

A new type of microsystem assembly was demonstrated using mechanical interfacing between interchangeable MEMS chips. Passive alignment elements and active interfacing from the UTP probe enabled mechanical actuation of test stages integrated in test coupon chips. The reuse of the same UTP chip was demonstrated through repeated placement, actuation, and removal of different test coupon chips. Compressive interfacing of structures experiencing in-plane motion on the UTP was demonstrated as an effective temporary mechanical interface to compliant structures on the test coupons. To achieve actuated interfacing, new thermally actuated MEMS manipulator probes were developed and operated in the UTP. Because of a compliant displacement amplification structure, actuation of 40 μm or greater was possible as mechanical output from this device.

Opportunities for future development include implementation of in-plane sensors and calibration of displacement and force measurements for application in mechanical testing. The use of a pick-and-place machine or a mechanical jig in order to achieve coupon assembly into the test platform should be explored as means to speed test setup and also to circumvent possible operator-induced microdevice damage. The microsystems developed here provide microfabricated laboratories for manipulating and interacting with microscale and nanoscale test objects. Other applications for this work beyond mechanical testing include stage actuators for microscale and nanoscale fabrication systems and compliant displacement amplification in nanoscale structures.

Acknowledgment

The authors would like to thank D. D. Luu (Sandia National Laboratory, formerly at the University of Colorado, Boulder) for the data acquisition system design. Electron microscopy was performed at the University of Colorado Nanomaterials Characterization Facility, Boulder. Fabrication was performed in collaboration with Dr. T. M. Wallis and Dr. P. Kabos at the NIST Boulder Quantum Fabrication Facility. Thermal coupon testing was performed at ETH Zürich through collaboration with Prof. C. Hierold and M. Muoth of the Micro and Nanosystems group.

References

[1] M. A. Haque, H. D. Espinosa, and H. J. Lee, "MEMS for *in situ* testing-handling, actuation, loading, and displacement measurements," *MRS Bull.*, vol. 35, no. 5, pp. 375–381, May 2010.

[2] R. Agrawal and H. D. Espinosa, "Multiscale experiments: State of the art and remaining challenges," *J. Eng. Mater. Technol.*, vol. 131, no. 4, p. 041 208, Oct. 2009.

[3] R. Agrawal, O. Loh, and H. D. Espinosa, "The evolving role of experimental mechanics in 1-D nanostructure-based device development," *Exp. Mech.*, vol. 51, no. 1, pp. 1–9, Jan. 2011.

[4] S. E. McCalla and A. Tripathi, "Microfluidic reactors for diagnostics applications," *Annu. Rev. Biomed. Eng.*, vol. 13, pp. 321–343, Aug. 2011.
[5] A. Webster, J. Greenman, and S. J. Haswell, "Development of microfluidic devices for biomedical and clinical application," *J. Chem. Technol. Biotechnol.*, vol. 86, no. 1, pp. 10–17, Jan. 2011.
[6] L. Wang and P. C. H. Li, "Microfluidic DNA microarray analysis: A review," *Anal. Chim. Acta*, vol. 687, no. 1, pp. 12–27, Feb. 2011.
[7] T. Kizuka, "Atomic process of point contact in gold studied by time-resolved high-resolution transmission electron microscopy," *Phys. Rev. Lett.*, vol. 81, no. 20, pp. 4448–4451, Nov. 1998.
[8] T. Kizuka, "Atomistic visualization of deformation in gold," *Phys. Rev. B, Condens. Matter*, vol. 57, no. 18, pp. 11 158–11 163, May 1998.
[9] M. A. Haque and M. T. A. Saif, "Application of MEMS force sensors for *in situ* mechanical chararacterization of nano-scale thin films in SEM and TEM," *Sens. Actuators A, Phys.*, vol. 97/98, no. 1/2, pp. 239–245, Apr. 2002.
[10] M. A. Haque and M. T. A. Saif, "Deformation mechanisms in free-standing nanoscale thin films: A quantitative *in situ* transmission electron microscope study," *Proc. Nat. Acad. Sci.*, vol. 101, no. 17, pp. 6335–6340, Apr. 2004.
[11] M. A. Haque and M. T. A. Saif, "*In situ* tensile testing of nanoscale freestanding thin films inside a transmission electron microscope," *J. Mater. Res.*, vol. 20, no. 7, pp. 1769–1777, 2005.
[12] H. Tamura, K. Nishii, H. Minoda, Y. Tanishiro, and K. Yagi, "Studies of surface stress by reflection electron microscopy and transmission electron microscopy," *Surf. Sci.*, vol. 357/358, no. 1–3, pp. 576–580, Jun. 1996.
[13] M. A. Verheijen, J. J. T. M. Donkers, J. F. P. Thomassen, J. J. van den Broek, R. A. F. van der Rijt, M. J. J. Dona, and C. M. Smit, "Transmission electron microscopy specimen holder for simultaneous *in situ* heating and electrical resistance measurements," *Rev. Sci. Instrum.*, vol. 75, no. 2, pp. 426–429, Feb. 2004.
[14] M. Zhang, E. A. Olson, R. D. Twesten, J. G. Wen, L. H. Allen, I. M. Robertson, and I. Petrov, "*In situ* transmission electron microscopy studies enabled by microelectromechanical system technology," *J. Mater. Res.*, vol. 20, no. 7, pp. 1802–1807, 2005.
[15] T. Kizuka, Y. Takatani, K. Asaka, and R. Yoshizaki, "Measurements of the atomistic mechanics of single crystalline silicon wires of nanometer width," *Phys. Rev. B, Condens. Matter*, vol. 72, no. 3, p. 035 333, Jul. 2005.
[16] A. Nafari, A. Danilov, H. Rodjegard, P. Enoksson, and H. Olin, "A micromachined nanoindentation force sensor," *Sens. Actuators A, Phys.*, vol. 123/124, pp. 44–49, Sep. 2005.
[17] M. S. Bobji, C. S. Ramanujan, J. B. Pethica, and B. J. Inkson, "A miniaturized TEM nanoindenter for studying material deformation *in situ*," *Meas. Sci. Technol.*, vol. 17, no. 6, pp. 1324–1329, Jun. 2006.
[18] M. Nakajima, F. Arai, and T. Fukuda, "*In situ* measurement of Young's modulus of carbon nanotubes inside a TEM through a hybrid nanorobotic manipulation system," *IEEE Trans. Nanotechnol.*, vol. 5, no. 3, pp. 243–248, May 2006.
[19] Y. Zhu and H. D. Espinosa, "An electromechanical material testing system for *in situ* electron microscopy and applications," *Proc. Nat. Acad. Sci.*, vol. 102, no. 41, pp. 14 503–14 508, Oct. 2005.
[20] M. Muoth, S.-W. Lee, and C. Hierold, "Platform for strainable, TEM-compatible, MEMS-embedded carbon nanotube transistors," in *Proc. IEEE MEMS*, Cancun, Mexico, Jan. 2011, pp. 83–86.
[21] J. J. Brown, A. I. Baca, K. A. Bertness, D. A. Dikin, R. S. Ruoff, and V. M. Bright, "Tensile measurement of single crystal gallium nitride nanowires on MEMS test stages," *Sens. Actuators A, Phys.*, vol. 166, no. 2, pp. 177–186, Apr. 2011.
[22] M. T. A. Saif and N. C. MacDonald, "A millinewton microloading device," *Sens. Actuators A, Phys.*, vol. 52, no. 1, pp. 65–75, Mar. 1996.
[23] M. T. A. Saif and N. C. MacDonald, "Measurement of forces and spring constants of microinstruments," *Rev. Sci. Instrum.*, vol. 69, no. 3, pp. 1410–1422, Mar. 1998.
[24] P. A. Williams, S. J. Papadakis, M. R. Falvo, A. M. Patel, M. Sinclair, A. Seeger, A. Helser, R. M. Taylor, S. Washburn, and R. Superfine, "Controlled placement of an individual carbon nanotube onto a microelectromechanical structure," *Appl. Phys. Lett.*, vol. 80, no. 14, pp. 2574–2576, Apr. 2002.
[25] M. Kiuchi, Y. Isono, S. Sugiyama, T. Morita, and S. Matsui, "Mechanical and electrical properties evaluation of carbon nanowire using electrostatic actuated nano tensile testing devices (EANAT)," in *Proc. 5th IEEE Conf. Nanotechnol.*, Nagoya, Japan, Jul. 2005, vol. 2, pp. 486–489.
[26] D. Zhang, J.-M. Breguet, R. Clavel, L. Phillippe, I. Utke, and J. Michler, "*In situ* tensile testing of individual Co nanowires inside a scanning electron microscope," *Nanotechnology*, vol. 20, no. 36, p. 365 706, Sep. 2009.
[27] S. Lu, D. A. Dikin, S. L. Zhang, F. T. Fisher, J. Lee, and R. S. Ruoff, "Realization of nanoscale resolution with a micromachined thermally actuated testing stage," *Rev. Sci. Instrum.*, vol. 75, no. 6, pp. 2154–2162, Jun. 2004.
[28] B. Peng, Y. Zhu, I. Petrov, and H. Espinosa, "A microelectromechanical system for nano-scale testing of one dimensional nanostructures," *Sens. Lett.*, vol. 6, no. 1, pp. 1–12, Feb. 2008.
[29] C. Stampfer, A. Jungen, R. Linderman, D. Obergfell, S. Roth, and C. Hierold, "Nano-electromechanical displacement sensing based on single-walled carbon nanotubes," *Nano Lett.*, vol. 6, no. 7, pp. 1449–1453, Jul. 2006.
[30] C. Stampfer, A. Jungen, and C. Hierold, "Fabrication of discrete nanoscale force sensors based on single-walled carbon nanotubes," *IEEE Sensors J.*, vol. 6, no. 3, pp. 613–617, Jun. 2006.
[31] A. V. Desai and M. A. Haque, "Test bed for mechanical characterization of nanowires," *Proc. IMechE, Part N, J. Nanoeng. Nanosyst.*, vol. 219, no. 2, pp. 57–65, Jan. 2005.
[32] J. Chung, K. Lee, J. Lee, and R. Ruoff, "Toward large-scale integration of carbon nanotubes," *Langmuir*, vol. 20, no. 8, pp. 3011–3017, Apr. 2004.
[33] A. Motayed, M. He, A. V. Davydov, J. Melngailis, and S. N. Mohammad, "Realization of reliable GaN nanowire transistors utilizing dielectrophoretic alignment technique," *J. Appl. Phys.*, vol. 100, no. 11, p. 114 310, Dec. 2006.
[34] J. S. Han and M. T. A. Saif, "*In situ* microtensile stage for electromechanical characterization of nanoscale freestanding films," *Rev. Sci. Instrum.*, vol. 77, no. 4, p. 045 102, Apr. 2006.
[35] M.-F. Yu, O. Lourie, M. J. Dyer, K. Moloni, T. F. Kelly, and R. S. Ruoff, "Strength and breaking mechanism of multiwalled carbon nanotubes under tensile load," *Science*, vol. 287, no. 5453, pp. 637–640, Jan. 2000.
[36] X. M. H. Huang, R. Caldwell, L. Huang, S. C. Jun, M. Huang, M. Y. Sfeir, S. P. O'Brien, and J. Hone, "Controlled placement of individual carbon nanotubes," *Nano Lett.*, vol. 5, no. 7, pp. 1515–1518, Jul. 2005.
[37] J. Hone, P. Kim, X. M. H. Huang, B. Chandra, R. Caldwell, J. Small, B. H. Hong, T. Someya, L. Huang, S. O'Brien, and C. P. Nuckolls, "Growth of nanotubes and chemical sensor applications," in *Proc. SPIE—Nanosensing Materials and Devices*, Dec. 2004, vol. 5593, pp. 1–12.
[38] A. Jungen, C. Stampfer, J. Hoetzel, V. M. Bright, and C. Hierold, "Process integration of carbon nanotubes into microelectromechanical systems," *Sens. Actuators A, Phys.*, vol. 130/131 (SPEC. ISS.), pp. 588–594, Aug. 2006.
[39] C. Yu, L. Shi, Z. Yao, D. Li, and A. Majumdar, "Thermal conductance and thermopower of an individual single-wall carbon nanotube," *Nano Lett.*, vol. 5, no. 9, pp. 1842–1846, Sep. 2005.
[40] Coventor, Inc., Cary, NC. [Online]. Available: http://www.coventor.com
[41] Tanner Research, Inc., Monrovia, CA, [Online]. Available: http://www.tanner.com
[42] D. D. Luu, "Instrumentation interfacing for MEMS mechanical test systems," M.S. thesis, Dept. Mech. Eng., Univ. Colorado, Boulder, CO, May 2010.
[43] H. D. Espinosa, Y. Zhu, and N. Moldovan, "Design and operation of a MEMS-based material testing system for nanomechanical characterization," *J. Microelectromech. Syst.*, vol. 16, no. 5, pp. 1219–1231, Oct. 2007.
[44] J. Gaspar, M. E. Schmidt, J. Held, and O. Paul, "Wafer-scale microtensile testing of thin films," *J. Microelectromech. Syst.*, vol. 18, no. 5, pp. 1062–1076, Oct. 2009.

Joseph J. Brown (M'03) received the A.B. degree in engineering sciences from Dartmouth College, Hanover, NH, in 2000, and the M.S. and Ph.D. degrees in mechanical engineering from the University of Colorado, Boulder, in 2008 and 2010, respectively.

In 2004, he helped found carbon nanotube manufacturer NanoComp Technologies, Inc., Concord, NH, and served there as a Senior Engineer until 2006. He is currently a Research Associate in the Department of Mechanical Engineering, University of Colorado, Boulder. He has published four refereed journal papers and two conference papers, and he is an inventor on three U.S. patents. His research interests center on precision assembly, mechanical characterization, applications of nanostructures and nanoscale systems, and the interface of materials technologies and MEMS design.

Dr. Brown was a recipient of a 2007 National Science Foundation Graduate Research Fellowship.

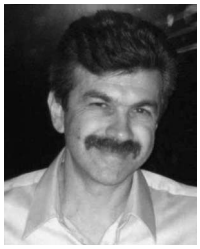

Dmitriy A. Dikin received the Ph.D. degree from the Institute for Low Temperature Physics and Engineering, Kharkov, Ukraine, in 1992.

From 1992 to 1993, he was a Postdoctoral Fellow with the Physics Institute, University of Würsburg, Germany. He is currently a Research Professor at Northwestern University, Evanston, IL. He is a coauthor of more than 70 refereed journal articles in the fields of physics, mechanics, and materials science. His research activities include study of physical and mechanical properties of nanotubes and nanowires, graphenes, nanocomposites by using low-noise electrical measurements, ultralow- and variable-temperature measurements, electron and scanning probe microscopy, and surface analysis.

Rodney S. Ruoff received the B.S. degree in chemistry from the University of Texas, Austin, and the Ph.D. degree from the University of Illinois, Urbana, in 1988.

He was a Fulbright Fellow with the Max Planck Institute, Goettingen, Germany. He is currently a Member of the Faculty at the University of Texas, Austin, where he serves as a Cockrell Family Regents Chair in mechanical engineering. He has published more than 250 refereed journal articles. His research activities include global environment and energy; synthesis and physical/chemical properties of nanostructures and composites; and nanorobotics, NEMS, and new tools for biomedical research.

Prof. Ruoff currently serves on the Editorial Board of the IEEE TRANSACTIONS ON NANOTECHNOLOGY.

Victor M. Bright (S'89–M'92–SM'07) received the B.S.E.E. degree from the University of Colorado, Denver, in 1986, and the M.S. and Ph.D. degrees from the Georgia Institute of Technology, Atlanta, in 1989 and 1992, respectively.

From 1992 to 1997, he was a Professor in the Department of Electrical and Computer Engineering, Air Force Institute of Technology, Wright-Patterson Air Force Base, OH. During 2004, he was a Visiting Professor at the Swiss Federal Institute of Technology (ETH Zürich), Zürich, Switzerland. From 2005 to 2007, he served as the Associate Dean for Research, College of Engineering and Applied Science (CEAS), University of Colorado, Boulder. He is currently the Alvah and Harriet Hovlid Professor and Chair of the Department of Mechanical Engineering, and the Faculty Director for Discovery Learning, CEAS, at the University of Colorado, Boulder. He is the author of over 90 archived journal papers in the fields of MEMS, NEMS, and microsystems. His research activities include MEMS and NEMS; silicon micromachining; microsensors/microactuators; optical, magnetic, and RF microsystems; atomic-layer deposited materials; ceramic MEMS; MEMS reliability; and MEMS packaging.

Prof. Bright is a Fellow of the American Society of Mechanical Engineers (ASME). He has served on the Executive Committee of the ASME MEMS Division, on the Technical Program Committee of the IEEE MEMS 2000–2006 conferences, and as the General Cochair for the IEEE MEMS 2005 International Conference. He also served on the Technical Program Committees for Transducers'03, Transducers'07, IEEE/LEOS Optical MEMS 2003–2005, and Hilton Head 2008 Solid-State Sensors and Actuators Workshop. He taught a short course on MEMS packaging at Transducers'03 and Transducers'05.